Simple permutation-based measure of quantum correlations and maximally-3-tangled states

Udaysinh T. Bhosale*
Indian Institute of Science Education and Research, Dr. Homi Bhabha Road, Pashan, Pune, 411 008, India

Arul Lakshminarayan†
Max-Planck-Institut für Physik komplexer Systeme, Nöthnitzer Straße 38, 01187 Dresden, Germany
and Department of Physics, Indian Institute of Technology Madras, Chennai, 600036 India

(Received 16 October 2015; revised manuscript received 10 March 2016; published 31 August 2016)

Quantities invariant under local unitary transformations are of natural interest in the study of entanglement. This paper deduces and studies a particularly simple quantity that is constructed from a combination of two standard permutations of the density matrix, namely, realignment and partial transpose. This bipartite quantity, denoted here as R_{12}, vanishes on large classes of separable states including classical-quantum correlated states, while being maximum for only maximally entangled states. It is shown to be naturally related to the 3-tangle in three-qubit states via their two-qubit reduced density matrices. Upper and lower bounds on concurrence and negativity of two-qubit density matrices for all ranks are given in terms of R_{12}. Ansatz states satisfying these bounds are given and verified using various numerical methods. In the rank-2 case, it is shown that the states satisfying the lower bound on R_{12} versus concurrence define a class of three-qubit states that maximize the tripartite entanglement (the 3-tangle) given an amount of entanglement between a pair of them. The measure R_{12} is conjectured, via numerical sampling, to be always larger than the concurrence and negativity. In particular, this is shown to be true for the physically interesting case of X states.

DOI: 10.1103/PhysRevA.94.022344

I. INTRODUCTION

Quantum entanglement, the nonlocal and unique feature of quantum mechanics, has been extensively investigated in the recent past, and forms an important part of quantum information theory [1]. In particular, shared bipartite entanglement is a crucial resource for many quantum information tasks such as teleportation [2], quantum cryptography [3], entanglement swapping [4,5], remote state preparation [6], dense coding [7], channel discrimination [8], and quantum repeaters [9]. Given a quantum state of many particles, say ρ, quantifying its entanglement content is naturally important. This question has been settled in favor of the von Neumann entropy of the reduced density matrices in the case of pure bipartite states [10], as it quantifies the entanglement that can be concentrated using local operations alone. In the case of two-qubit states, mixed or pure, "concurrence" is used, as it was shown to be a monotonic function of the entanglement of formation [11–13].

The partial transpose (PT) introduced by Peres [14] is a powerful and simple tool to detect entanglement in mixed bipartite states. However, while positivity under partial transpose is necessary for separability, it fails to detect a class of entangled states the so-called bound entangled states [15]. Nevertheless, the logarithmic negativity [16] measure based on the partial transpose is a useful measure of entanglement in mixed states. More general measures of quantum correlation, such as the quantum discord [17,18], have been extensively studied as well. These measures of correlations can be nonzero for states that have no entanglement content.

The purpose of this work is to focus on a measure that uses a simple permutation of the density matrix. Given the multitude of entanglement and correlation measures, this work seeks to highlight some of the unique properties of this quantity such as its vanishing on classically correlated states and its natural relationship with concurrence and the three-tangle. It is seen as a natural quantity when considering the problem of maximizing the 3-tangle of three-qubit states given a fixed entanglement between two of them. This gives rise to an interesting set of states that we refer to as maximally 3-tangled states. Thus, it is likely that this measure, which can be easily calculated for any state, has physical content that deserves further exploration.

Any measure of entanglement can not increase under local operations and classical communications (LOCC) and it should be constant and minimal on all separable states [1,19]. This also implies that the measure of entanglement must be invariant under local unitary (LU) transformations. The spectra of the density matrix itself and the various reduced density matrices got by tracing out subsystems are such LU invariants. They could be invariant under nonlocal operations and therefore their interpretation in terms of entanglement is generally not tenable. However, interestingly, if the single subsystem reduced density matrices of a multipartite pure state are considered, collection of their eigenvectors form convex polytopes that characterize distinct entanglement classes [20–22]. Here, the notion of entanglement class is a broader class than LU, and includes measurements and classical communications, that are included in the operation known as stochastic local operations and classical communications (SLOCC). It is clear that states that cannot be converted to each other by LU are also not SLOCC equivalent, but the converse is not true. States that can be converted to each other by SLOCC are from an entanglement class. In the case of three-qubit pure states, there are two different entanglement classes, known

*udaybhosale0786@gmail.com
†arul@physics.iitm.ac.in

as the W and the GHZ, while for four qubits there are nine [23].

Given a bipartite system 1 and 2 having a product orthonormal basis $\{|i\rangle|\alpha\rangle\}$ and density matrix ρ_{12}, the PT with respect to the second subsystem, denoted as $\rho_{12}^{T_2}$, is given by the matrix elements

$$\left(\rho_{12}^{T_2}\right)_{i\alpha;j\beta} = (\rho_{12})_{i\beta;j\alpha}; \quad (\rho_{12})_{i\alpha;j\beta} = \langle i|\langle\alpha|\rho_{12}|j\rangle|\beta\rangle. \quad (1)$$

Peres's partial transpose criterion states that if $\rho_{12}^{T_2}$ is negative, then the state ρ_{12} is entangled. The other operation of interest to this work is realignment [24,25]. The corresponding operation on the density matrix ρ_{12}, denoted as $\mathcal{R}(\rho_{12})$, is given by

$$\langle i|\langle j|(\mathcal{R}(\rho_{12}))|\alpha\rangle|\beta\rangle = \langle i|\langle\alpha|\rho_{12}|j\rangle|\beta\rangle. \quad (2)$$

The realignment criterion is that if the state ρ_{12} is separable, then $\|\mathcal{R}(\rho_{12})\|_1 \leqslant 1$, where $\|M\|_1$ is the trace norm equal to $\mathrm{tr}\sqrt{MM^\dagger}$ [26]. This condition is found to detect some bound entangled states, these being positive under PT and hence not being detected by the corresponding criterion [15,25]. Note that both the realignment and partial transpose are simple permutations of the elements of the density matrix. While the partial transpose retains the Hermiticity of the operator, realignment does not. In fact, if the subsystems are of different dimensionalities, it results in a rectangular matrix.

Consider a system consisting of M subsystems labeled by i $(1 \leqslant i \leqslant M)$, each in a Hilbert space of dimension d_i. If its joint state is ρ, it was shown in [27], motivated by considerations in [28], that LU invariants could be constructed in the following way. Let $\{a\} = (i_1, i_2, \ldots, i_K)$ be an arbitrary *closed* path in the space of labels of the subsystems, that is, $1 \leqslant i_k \leqslant M$ and $i_{K+1} = i_1$. Then, the eigenvalues of

$$\mathcal{P}(\{a\}) = \mathcal{R}\left(\rho_{i_1 i_K}^{T_{i_K}}\right) \ldots \mathcal{R}\left(\rho_{i_2 i_1}^{T_{i_1}}\right) \quad (3)$$

are (in general complex) LU invariants. Here, $\rho_{i_k i_m}$ is a bipartite state obtained by tracing out all other subsystems except i_k and i_m. It was also shown in [27] that the characteristic polynomial of $\mathcal{P}$ is real and hence these real coefficients are also LU invariants. Note that the "link transformation" [27,28] is a combination of both PT and realignment, executed in that order.

In the same work [27], it was shown that for the case of bipartite pure state of two qubits, the quantity $\det[\mathcal{R}(\rho_{12}^{T_2})\mathcal{R}(\rho_{21}^{T_1})]^{1/4}$ is equal to $\tau_2/4$, where τ_2 is the two-tangle [29], i.e., square of the concurrence [11–13]. This motivates the question of the meaning of the spectra of $\mathcal{R}(\rho_{12}^{T_2})$ as entanglement or correlation measures in an arbitrary bipartite system. Using this, a new and central quantity of this paper is defined and investigated in the case of two-qubit density matrices of general rank.

The structure of the paper is as follows: In Sec. II, the measure is defined and basic properties are studied, along with its evaluation for various classes of states. In Sec. III, two-qubit states of rank 2 or equivalently three-qubit pure states are studied in detail. Bounds for the concurrence are given in terms of the defined measure. Various boundaries of the inequality are characterized and two classes of maximally-3-tangled states are discussed. The difference between the concurrence and the measure is shown to have direct connections with the tripartite measure of the 3-tangle. In Sec. IV, results on two-qubit states of rank greater than 2 are presented. Rank-3 and rank-4 boundaries are also investigated and all of these are found to be Bell-diagonal states. The measure is also evaluated for a special class of states, namely the X states, and is shown to be larger than the concurrence. In Sec. V, negativity is compared with R_{12} and again various boundaries are investigated and their significance pointed out when we can. For example, in this case the MEMS I states lie on the boundary for rank-2 states. The Werner states and pure states form common outer boundaries in both the R_{12}-concurrence and R_{12}-negativity comparisons.

II. A SIMPLE LU INVARIANT FROM REALIGNMENT AND PARTIAL TRANSPOSE

As discussed above, products of certain permutations of bipartite density matrices along a path in the space of labels are capable of generating LU invariants. This paper is mainly devoted to exploring the simplest of these, namely, when the path simply connects two subsystems: say $1 \to 2 \to 1$. The operator in this case is $\mathcal{P}(12) = \mathcal{R}(\rho_{12}^{T_2})\mathcal{R}(\rho_{21}^{T_1}) = \mathcal{R}(\rho_{12}^{T_2})\mathcal{R}(\rho_{12}^{T_2})^\dagger$, and hence is positive. While all the eigenvalues or the coefficients of the characteristic polynomial of $\mathcal{P}(12)$ maybe considered, in this paper the quantity

$$R_{12} = d\,\{\det[\mathcal{P}(12)]\}^{1/2d^2} = d\left\{\left|\det\left[\mathcal{R}\left(\rho_{12}^{T_2}\right)\right]\right|\right\}^{1/d^2} \quad (4)$$

is studied. In particular, the case $d_1 = d_2 = d$ is considered so that the array $\mathcal{R}(\rho_{12}^{T_2})$ is square. Else, straightforward generalized forms need to be used. The somewhat strange power is to make contact with the well-known entanglement measure of concurrence when $d = 2$, a case that we will almost exclusively consider. From the definition it is obvious that R_{12}/d is the geometric mean of the singular values of $\mathcal{R}(\rho_{12}^{T_2})$.

This quantity contains the entanglement along with other correlations that may come from multipartite entanglement of purifications of ρ_{12}. Various evidences for this fact will be presented in the subsequent parts of the paper. To be precise, it is shown that for various classes of states R_{12} exceeds or equals well-known measures of entanglement which shows that the term ρ_{12} captures other correlations along with entanglement. It is interesting to note that in the case of two qubits, R_{12} is equal to the volume of a steering ellipsoid [30–32], also called "obesity," which arises in the quantum steering ellipsoid formalism of two-qubit states. The quantum steering ellipsoid of a two-qubit state is defined as the set of Bloch vectors that Bob can collapse Alice's qubit to, considering all possible measurements on his qubit. This formalism has provided a faithful and intuitive representation of two-qubit states. This observation gives an operational meaning to the term R_{12} that needs further exploration.

The letter R is used to signify this quantity and maybe considered as some sort of "rapprochement" between the two subsystems. As the partial transpose followed by realignment is repeatedly done in the following, it is useful to show their combined operation explicitly in the case of a two-qubit

state:

$$\rho = \begin{pmatrix} a_{11} & a_{12} & a_{13} & a_{14} \\ a_{12}^* & a_{22} & a_{23} & a_{24} \\ a_{13}^* & a_{23}^* & a_{33} & a_{34} \\ a_{14}^* & a_{24}^* & a_{34}^* & a_{44} \end{pmatrix}$$

$$\mapsto \mathcal{R}(\rho^{T_2}) = \begin{pmatrix} a_{11} & a_{12}^* & a_{12} & a_{22} \\ a_{13} & a_{23} & a_{14} & a_{24} \\ a_{13}^* & a_{14}^* & a_{23}^* & a_{24}^* \\ a_{33} & a_{34}^* & a_{34} & a_{44} \end{pmatrix}. \tag{5}$$

For product states of the form $\rho_{12} = \rho_1 \otimes \rho_2$, which is the special case of separable states, $\mathcal{R}(\rho_{12}^{T_2})$ is a rank-1 projector. The crucial observation is that for such product states

$$\mathcal{R}\left(\rho_{12}^{T_2}\right) = \rho_1^R \left(\rho_2^R\right)^\dagger, \tag{6}$$

where the notation $\rho_{1,2}^R$ denotes the density matrix reshaped into a column vector of dimension $d_{1,2}^2$ and $(\rho_{1,2}^R)^\dagger$ denotes the Hermitian conjugate of $\rho_{1,2}^R$. The reshaping is done by stacking the rows in a column. Therefore, $\mathcal{R}(\rho_{12}^{T_2})$ is a matrix of dimension $d_1^2 \times d_2^2$. To understand this more clearly, an example of two-qubits will be considered explicitly. Let ρ_1 and ρ_1 denote the density matrices of qubits 1 and 2, respectively, as follows:

$$\rho_1 = \begin{pmatrix} a_{11} & a_{12} \\ a_{12}^* & a_{22} \end{pmatrix} \quad \text{and} \quad \rho_2 = \begin{pmatrix} b_{11} & b_{12} \\ b_{12}^* & b_{22} \end{pmatrix}. \tag{7}$$

Then, $\rho_{1,2}^R$ are given as follows:

$$\rho_1^R = \begin{pmatrix} a_{11} \\ a_{12} \\ a_{12}^* \\ a_{22} \end{pmatrix} \quad \text{and} \quad \rho_2^R = \begin{pmatrix} b_{11} \\ b_{12} \\ b_{12}^* \\ b_{22} \end{pmatrix}. \tag{8}$$

Using Eq. (6), one obtains the following: This implies that

$$\rho_1^R (\rho_2^R)^\dagger = \begin{pmatrix} a_{11}b_{11} & a_{11}b_{12}^* & a_{11}b_{12} & a_{11}b_{22} \\ a_{12}b_{11} & a_{12}b_{12}^* & a_{12}b_{12} & a_{12}b_{22} \\ a_{12}^*b_{11} & a_{12}^*b_{12}^* & a_{12}^*b_{12} & a_{12}^*b_{22} \\ a_{22}b_{11} & a_{22}b_{12}^* & a_{22}b_{12} & a_2b_{22} \end{pmatrix} \tag{9}$$

and is easily seen to be $\mathcal{R}(\rho_1 \otimes \rho_2^T)$.

For two-qubit pure states it is easy to see that [27] $R_{12} = C_{12}$, where C_{12} is the concurrence [11–13]. Thus, this motivates a more detailed study of this quantity in the case of higher-rank two-qubit density matrices and its relationship to the concurrence. R_{12} is a symmetric measure, i.e., $R_{12} = R_{21}$, when the subsystems have equal dimensions. This follows from the definition, R_{12} depends on the eigenvalues of $\mathcal{R}(\rho_{12}^{T_2})\mathcal{R}(\rho_{21}^{T_1})$, while R_{21} depends on the eigenvalues of $\mathcal{R}(\rho_{21}^{T_1})\mathcal{R}(\rho_{12}^{T_2})$. These two sets of eigenvalues can differ only in the number of zero eigenvalues, which happens when the subsystem dimensions are different. Hence, we may define R_{12} to be such that subsystem labeled 1 is not of larger dimension than that of subsystem 2.

The following proposition is now proved:

Proposition 1. $0 \leqslant R_{12} \leqslant 1$.

Proof. Let the eigenvalues of $\mathcal{P}(12) = \mathcal{R}(\rho_{12}^{T_2})\mathcal{R}(\rho_{12}^{T_2})^\dagger$ be μ_j, $1 \leqslant j \leqslant d^2$. Then,

$$R_{12} = d\left(\prod_{j=1}^{d^2} \sqrt{\mu_j}\right)^{1/d^2} \leqslant \frac{1}{d}\sum_{j=1}^{d^2} \sqrt{\mu_j}, \tag{10}$$

which follows from the fact that geometric mean is no larger than the arithmetic mean. As $\mathcal{R}(\rho_{12}^{T_2})$ is only a permutation of the original density matrix, it follows that $\mathrm{tr}[\mathcal{P}(12)] = \sum_{j=1}^{d^2} \mu_j = \mathrm{tr}(\rho_{12}^2) \leqslant 1$. An application of the Cauchy-Schwarz inequality $\sum_i a_i b_i \leqslant \sqrt{\sum_i a_i^2}\sqrt{\sum_i b_i^2}$, with $a_i = \sqrt{\mu_i}$, $b_i = 1$, gives $\sum_{j=1}^{d^2} \sqrt{\mu_j} \leqslant d$, which results in $R_{12} \leqslant 1$ as required. The lower limit is evident. ■

It is instructive to evaluate R_{12} for well-known classes of states and therefore the following examples are considered.

(1) *Bipartite pure states.* Using Schmidt decomposition every bipartite pure state can always be written as $|\psi_{12}\rangle = \sum_{k=1}^{d} \sqrt{\lambda_k}|\phi_k\rangle|\psi_k\rangle$ where $d = \min\{d_1, d_2\}$. It follows that $\mathcal{R}(|\psi_{12}\rangle\langle\psi_{12}|^{T_2}) =$

$$\sum_{k,j} \sqrt{\lambda_j\lambda_k}|\phi_j\rangle|\phi_k\rangle\langle\psi_k|\langle\psi_j|. \tag{11}$$

The eigenvalues of $\mathcal{P}(12)$ are then $\lambda_k\lambda_j$ for $k, j = 1, 2, \ldots, d$ which gives

$$R_{12} = d\left(\prod_{k}^{d} \lambda_k\right)^{1/d}.$$

For maximally entangled states $\lambda_k = 1/d \;\forall\; k$, and it follows that $R_{12} = 1$. This also follows from the fact that the maximally entangled state $\sum_{j=1}^{d} |jj\rangle/\sqrt{d}$ gives $\mathcal{R}(\rho_{12}^{T_2}) = S_{12}/d$, where S_{12} is the swap operator $S_{12}|ij\rangle = |ji\rangle$.

(2) *Bell-diagonal states.* These states, as the name suggests, are diagonal in the Bell basis [12,33]:

$$\rho_{12} = p_1|\phi^+\rangle\langle\phi^+| + p_2|\psi^+\rangle\langle\psi^+| + p_3|\psi^+\rangle\langle\psi^+| + p_1|\phi^-\rangle\langle\phi^-|,$$

where $\sum_i^4 p_i = 1$, and $|\psi^\pm\rangle = (1/\sqrt{2})(|01\rangle + |10\rangle)$ while $|\phi^\pm\rangle = (1/\sqrt{2})(|00\rangle + |11\rangle)$. This state is separable iff its spectrum lies in [0,1/2] [34], otherwise it is entangled. The entanglement calculated using the concurrence is $C_{12} = \max\{0, 2p_{\max} - 1\}$ [13] where $p_{\max} = \max\{p_1, p_2, p_3, p_4\}$. It is a simple calculation to show that

$$R_{12} = |8(p_2 + p_3 - 1/2)(p_2 + p_4 - 1/2)(p_3 + p_4 - 1/2)|^{1/4}$$

and is nonzero even when concurrence is zero. In fact, R_{12} is zero for any pair of p_i and p_j $(i \neq j)$ satisfying $p_i + p_j = 1/2$. Bell-diagonal states appear as boundaries in many of the following phase diagrams, and one special case of it, the Werner state, is worth singling out for further details.

(3) *Werner state.* A well-known mixture of the maximally entangled and mixed state is the two-qubit Werner state: $\rho_{12} = (1 - p)I/4 + p\,|\phi^+\rangle\langle\phi^+|$ [35] where p $(0 \leqslant p \leqslant 1)$. This state is entangled iff $1/3 \leqslant p \leqslant 1$ and in that case

the entanglement, as measured by the concurrence, is $C_{12} = (3p-1)/2$. It is readily seen, however, that $R_{12} = p^{3/4}$, and hence is nonzero when the concurrence is zero, except in the extreme case of $p = 0$, when there is a maximally mixed state. It is easy to see that $p^{3/4} - (3p-1)/2$ is monotonically decreasing in $[1/3, 1]$ and hence attains the minimum value of 0 at $p = 1$. This implies that $R_{12} \geqslant C_{12}$ for all values of p, equality occurring only at the extreme cases of $p = 0$ and 1.

(4) *Maximally entangled mixed states (MEMS).* These states [33,36–39] are two-qubit states whose entanglement (concurrence) is maximized for a given value of mixedness, measured using linear entropy. These states have been realized experimentally [39] using correlated photons from parametric down-conversion. There are two classes of MEMS, the rank-2 (MEMS I) and rank-3 (MEMS II) ones and are given as follows:

$$\rho_{\text{MEMS I}} = \begin{pmatrix} C_{12}/2 & 0 & 0 & C_{12}/2 \\ 0 & 1-C_{12} & 0 & 0 \\ 0 & 0 & 0 & 0 \\ C_{12}/2 & 0 & 0 & C_{12}/2 \end{pmatrix}, \quad \text{where} \quad \frac{2}{3} \leqslant C_{12} \leqslant 1 \tag{12}$$

and

$$\rho_{\text{MEMS II}} = \begin{pmatrix} 1/3 & 0 & 0 & C_{12}/2 \\ 0 & 1/3 & 0 & 0 \\ 0 & 0 & 0 & 0 \\ C_{12}/2 & 0 & 0 & 1/3 \end{pmatrix}, \quad \text{where} \quad 0 \leqslant C_{12} \leqslant \frac{2}{3}, \tag{13}$$

respectively. It readily follows from the definition in Eq. (4) that $R_{12} = C_{12}$ for MEMS I and $R_{12} = \sqrt{2C_{12}/3}$ for MEMS II for the respective ranges of C_{12}. It is easy to see $\sqrt{2C_{12}/3} - C_{12} \geqslant 0$ in the range $0 \leqslant C_{12} \leqslant 2/3$, equality occurring only at $C_{12} = 0$ and $2/3$. This implies that $R_{12} \geqslant C_{12}$ for MEMS. We will see below that this inequality is of general validity.

(5) *Separable states.* Consider first product states of the form $\rho_{12} = \rho_1 \otimes \rho_2$. Using Eq. (6) one obtains the following:

$$\begin{aligned} \mathcal{P}(12) &= \mathcal{R}\big(\rho_{12}^{T_2}\big)\mathcal{R}\big(\rho_{21}^{T_1}\big) = \mathcal{R}\big(\rho_{12}^{T_2}\big)\mathcal{R}\big(\rho_{12}^{T_2}\big)^\dagger \\ &= \rho_1^R\big(\rho_2^R\big)^\dagger\rho_2^R\big(\rho_1^R\big)^\dagger = \operatorname{tr}\big(\rho_2^2\big)\rho_1^R\big(\rho_1^R\big)^\dagger \end{aligned} \tag{14}$$

which is of rank 1 and hence $R_{12} = 0$.

For states of the form $\rho_{12} = \sum_{k=1}^{M} p_k \rho_{1k} \otimes \rho_{2k}$, a similar calculation yields

$$\mathcal{P}(12) = \sum_{k,l=1}^{M} p_k p_l \operatorname{tr}(\rho_{2k}\,\rho_{2l})\rho_{1k}^R\big(\rho_{1l}^R\big)^\dagger. \tag{15}$$

This cannot be of full rank if $M < d_1^2$, and hence $R_{12} = 0$ in this case as well.

(6) *Classical-quantum correlated states.* These are of the form [40–42]

$$\rho_{CQ} = \sum_i p_i\, |i\rangle\langle i| \otimes \rho_i, \tag{16}$$

where $\{|i\rangle\}$ are orthonormal and ρ_i are arbitrary states. In this and the next example we use subscripts C and Q for the subsystems so as to make the classical and quantum labels explicit. As a special case of separable states with $M \leqslant d_C < d_C^2$ it follows from Eq. (15) that $R_{CQ} = 0$. Alternatively, it is straightforward to verify that

$$\mathcal{P}(CQ) = \sum_{ij} \operatorname{tr}(\rho_i \rho_j) p_i p_j |ii\rangle\langle jj|,$$

and hence there are at least $d_C^2 - d_C$ vanishing eigenvalues of $\mathcal{P}(CQ)$, implying that $R_{CQ} = 0$. It should be noted that this is true irrespective of whether the dimension of the classical subsystem is greater or less than that of the quantum.

(7) *Quantum-classical correlated states.* From the symmetry property of R it may appear that we can conclude that it vanishes also for quantum-classical correlated states where the orthonormal projectors are in the second subspace. The nonzero eigenvalues of $\mathcal{P}(QC)$ are the same as that of $\mathcal{P}(CQ)$, which are at most d_C in number. Therefore, if $d_Q^2 \leqslant d_C$ we cannot conclude that $\mathcal{P}(QC)$ is rank deficient, and hence R_{QC} maybe nonzero in this case. On the other hand, if $d_Q^2 > d_C$ we can indeed conclude that $R_{QC} = 0$. This is related to the restriction on the number of product states in the general separable case considered in Eq. (15).

As a simple special case it also follows that R vanishes for all classical-classical correlated states. It is interesting that the quantum discord also vanishes for classical-classical states. In the case of classical-quantum correlated states, it vanishes only when the measurements are done on the classical part of the state, otherwise, it does not vanish in general. In fact, it vanishes iff the state is of this form and measurements are done on the classical part of the state [41]. The quantity R_{12} is a very simply calculable quantity unlike the quantum discord, and also vanishes for such states. Thus, R_{12} does not seem to include any correlations that are excluded by quantum discord.

Thus, for rank-1 two-qubit density matrix R_{12} gives entanglement. But, for higher ranks R_{12} contains not just entanglement but correlations of other types also. Since R_{12} is nonconstant and nonzero for separable states as seen in the case of separable Werner states, it is not an entanglement monotone [1,19]. But, since R_{12} equals concurrence for two-qubit pure states it is an entanglement monotone only on such states. In this respect, it is similar to the quantum discord [17,18,43] which includes other correlations and it almost never vanishes. Quantum discord too is not an entanglement monotone except on bipartite pure states since in this case it equals von Neumann entropy. However, of course, the discord has an information-theoretic interpretation of a difference of two types of mutual information. It will be seen below how the difference between R_{12} and C_{12} for rank-2 two-qubit states has a natural interpretation.

III. RANK-2 TWO-QUBIT DENSITY MATRICES OR PURE THREE-QUBIT STATES

Any rank-2 two-qubit density matrix can be obtained as a reduced density matrix of a suitable three-qubit pure state. In this section, the measure R_{12} is explored for such rank-2 density matrices with this intrinsic relationship to three-qubit states in mind. Three-qubit states (pure as well as mixed) have been actively explored in the recent past [29,44–56], as they offer the simplest system that includes multiparty entanglement sharing. Construction of LU invariants was

discussed in [46], however, the quantity R_{12} was not considered therein. A pure multipartite entanglement measure, the 3-tangle, was introduced in [29]. The archetypal states of GHZ and W were superposed and resulting entanglement studied in [48,49,51,57]. These were based on various entanglement measures such as concurrence, negativity, log-negativity, entanglement of formation, von Neumann entropy, squashed entanglement, and so on [1].

The canonical form of three-qubit pure states [45] is extremely useful and given by

$$|\psi\rangle = \lambda_0|000\rangle + \lambda_1 e^{i\theta}|100\rangle + \lambda_2|101\rangle + \lambda_3|110\rangle + \lambda_4|111\rangle, \tag{17}$$

where $\lambda_i \in [0,1]\ \forall\ i = 0$ to 4, $\sum_i \lambda_i^2 = 1$, and $\theta \in [0,\pi]$. It can be seen that Eq. (17) has only five independent parameters excluding the trace [46]. The general three-qubit state with 16 real parameters is reduced to these 5 by LU transforms that have $3 \times 3 = 9$ real parameters, and by accounting for overall normalization and phase. Thus, this is the minimal form of any such state. The following proposition for a two-qubit density matrix of rank 2 now follows.

Proposition 2. For a rank-2 two-qubit density matrix $R_{12}^2 \leqslant C_{12} \leqslant R_{12}$ or, equivalently, $C_{12} \leqslant R_{12} \leqslant \sqrt{C_{12}}$.

Proof. Using the canonical form of a three-qubit state which is a purification of the given state ρ_{12} leads to the following parametrization:

$$\rho_{12} = \begin{pmatrix} \lambda_0^2 & 0 & \lambda_0\lambda_1 e^{i\theta} & \lambda_0\lambda_3 \\ 0 & 0 & 0 & 0 \\ \lambda_0\lambda_1 e^{-i\theta} & 0 & \lambda_1^2+\lambda_2^2 & \lambda_1\lambda_3 e^{-i\theta}+\lambda_2\lambda_4 \\ \lambda_0\lambda_3 & 0 & \lambda_1\lambda_3 e^{i\theta}+\lambda_2\lambda_4 & \lambda_3^2+\lambda_4^2 \end{pmatrix}. \tag{18}$$

The following measures are readily calculated:

$$C_{12} = 2\lambda_0\lambda_3 \quad \text{and} \quad R_{12} = 2\lambda_0\lambda_3^{1/2}\left(\lambda_3^2+\lambda_4^2\right)^{1/4}. \tag{19}$$

Considering the difference

$$C_{12}^4 - R_{12}^4 = -16\lambda_0^4\lambda_3^2\lambda_4^2 \leqslant 0, \tag{20}$$

it follows that $C_{12} \leqslant R_{12}$.

Similarly,

$$\begin{aligned} R_{12}^4 - C_{12}^2 &= 4\lambda_0^2\lambda_3^2\left[4\lambda_0^2\left(\lambda_3^2+\lambda_4^2\right)-1\right] \\ &\leqslant 4\lambda_0^2\lambda_3^2\left[4\lambda_0^2\left(1-\lambda_0^2\right)-1\right] \leqslant 0, \end{aligned} \tag{21}$$

where the first inequality follows from $\lambda_3^2+\lambda_4^2 \leqslant 1-\lambda_0^2$, a consequence of the normalization constraint. The second follows from the fact that $x(1-x)$ attains the maximum value of $1/4$ when $0 \leqslant x \leqslant 1$. Thus, the proposition is proved. ■

The equality $R_{12} = C_{12}$ in the case of rank-1 two-qubit states becomes broadened into this inequality and the measure R_{12} is never smaller than concurrence in the case of rank-2 states. However, there is also an upper bound on R_{12}, as it is never larger than $\sqrt{C_{12}}$. Thus, C_{12} and R_{12} when they vanish do so simultaneously.

A. The 3-tangle, concurrence, and R_{12} in three-qubit pure states

The difference $R_{12}^4 - C_{12}^4$ is now shown to be related to the tripartite entanglement in the three-qubit purification, namely,

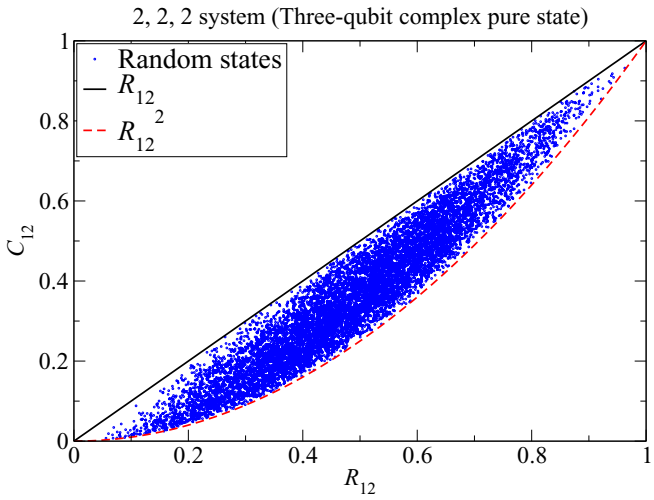

FIG. 1. The R_{12} and the entanglement between two qubits C_{12} having density matrix ρ_{12} of rank 2. Also shown are the bounds from proposition 2, the straight line being W states, while the parabola consists of maximally-3-tangled ones (M3TS). Here, 10 000 random tripartite complex three-qubit pure states are used.

the 3-tangle. To recall the definition of the 3-tangle [29], it is given by $\tau = C_{1(23)}^2 - C_{12}^2 - C_{13}^2$ where C_{ij} is the concurrence between qubits i and j. The quantity $C_{1(23)}$ is the concurrence between qubit 1 and the pair of qubits 2 and 3 since in the case of three-qubit pure state, the reduced density matrix of qubits 2 and 3 is of rank 2. The 3-tangle τ has been shown to be permutationally invariant and $0 \leqslant \tau \leqslant 1$. The expression of the 3-tangle is rather complicated, and can be expressed as a Cayley hyperdeterminant [29], however, in terms of the parameters of the canonical form it is simply $\tau = 4(\lambda_0\lambda_4)^2$. Along with Eq. (19) this leads to the remarkably simple relation

$$R_{12}^4 = C_{12}^2\left(C_{12}^2+\tau\right). \tag{22}$$

It can be seen that in the case of two-qubit rank-1 density matrices, i.e., two-qubit pure states where the 3-tangle (τ) is equal to zero, the equality above reduces to the one proved in [27], namely, $C_{12} = R_{12}$. From the point of purification it implies that if the two quantities C_{12} and R_{12} of a two-qubit density matrix are fixed, then after purification to a three-qubit pure state the 3-tangle (τ) of the final state also gets fixed and is given using Eq. (22) as follows:

$$\tau = \frac{R_{12}^4 - C_{12}^4}{C_{12}^2}. \tag{23}$$

It should be noted that the 3-tangle is permutation invariant and, hence, the combination in the right-hand side will inherit this property.

Figure 1 shows R_{12} versus concurrence between two qubits where the overall three-qubit state is randomly sampled according to the Haar measure. The relation between the two measures as reflected in the inequality of Proposition 2 is seen as the region bounding the straight line and the parabola. It is of interest to analyze the states that make up the boundaries of this region.

B. Upper boundary are from *W* states

The upper boundary in Fig. 1 corresponds to $C_{12} = R_{12}$. Using Eq. (19), this is seen to imply that $\lambda_4 = 0$ when the entanglement is nonzero. The corresponding states are therefore the W class of states [51]

$$|\psi\rangle = \lambda_0|000\rangle + \lambda_1 e^{i\theta}|100\rangle + \lambda_2|101\rangle + \lambda_3|110\rangle. \quad (24)$$

It is easy to calculate then that $C_{12} = R_{12} = 2\lambda_0\lambda_3$, $C_{13} = R_{13} = 2\lambda_0\lambda_2$, $C_{23} = R_{23} = 2\lambda_2\lambda_3$. The tripartite measure of entanglement, the 3-tangle simply denoted as τ, is 0 for all these states. Note that the relation in Eq. (22) implies that for the upper boundary indeed $\tau = 0$. Thus, the W class of states is similar to pure two-qubit states, inasmuch as there is no difference between the measure R_{12} and concurrence. W states maximize the concurrence between two qubits for a given R_{12}. This is reminiscent of states that maximize concurrence for a given purity, and indeed these are seen to be on the upper boundary too for the following reason.

1. *MEMS I is the reduced density matrix of W state*

It will be now shown that the MEMS I are reduced density matrices of W class states. In Sec. II it is shown that $R_{12} = C_{12}$ for MEMS I. Note that while the state above is an MEMS I state only in the range $2/3 \leqslant C_{12} \leqslant 1$, our use of it is the entire range $0 \leqslant C_{12} \leqslant 1$. Therefore, this state is continued to be referred to as "MEMS I" for convenience although strictly speaking it is a generalization that is no more maximally entangled when $C_{12} < 2/3$.

Using Eq. (22) it can be seen that if purification of MEMS I is carried out, in this case to a three-qubit pure state, then the 3-tangle of the purified state is equal to zero. In the earlier Sec. III B it was shown that $C_{ij} = R_{ij}$ for all pairs in W class of states having zero 3-tangle. This naturally raises the question of whether MEMS I are the reduced density matrices of W class of states. Indeed, it is found that for parameter values of $\lambda_0^2 = \lambda_3^2 = C_{12}/2$ and $\lambda_2^2 = 1 - C_{12}$ in Eq. (24) of W class of states, the reduced density matrix of the first and second qubits is that of MEMS I. The corresponding canonical form of the W state for which the reduced density matrix of the first and second qubits is MEMS I is

$$|\psi\rangle = \sqrt{\frac{C_{12}}{2}}|000\rangle + \sqrt{1 - C_{12}}|101\rangle + \sqrt{\frac{C_{12}}{2}}|110\rangle. \quad (25)$$

MEMS I states appear later in this paper, when negativity is discussed, as a very different boundary.

C. Lower boundary are from maximally-3-tangled states

The lower boundary of Fig. 1 is characterized by states that have $C_{12} = R_{12}^2$. Fixing the entanglement C_{12} between two qubits which are part of a three-qubit pure state, these maximize R_{12}. While this seems obscure, it is clear from Eq. (22) that for a given C_{12}, maximizing R_{12} is the same as maximizing the tripartite entanglement as measured by the 3-tangle. In this sense, the states that make up the lower boundary are maximally-3-tangled states (M3TS). Using Eq. (19), one derives that $C_{12} = R_{12}^2$ implies, provided $\lambda_3 \neq 0$, $\lambda_0 \neq 0$,

$$\lambda_0^4 - \lambda_0^2\left(1 - \lambda_1^2 - \lambda_2^2\right) + \tfrac{1}{4} = 0. \quad (26)$$

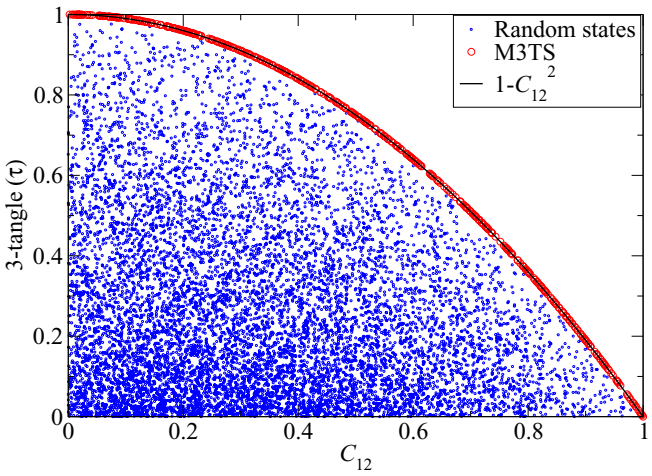

FIG. 2. The 3-tangle and the concurrence between first and second qubits (C_{12}) of a three-qubit pure state is shown. Here, 10 000 such states are sampled according to the uniform Haar measure. The M3TS states are selected from Eq. (27) where the value of the parameter C_{12} is chosen randomly.

This implies that $\lambda_1 = \lambda_2 = 0$, else the discriminant of the quadratic equation in λ_0^2 becomes negative. Hence,

$$\lambda_0 = \frac{1}{\sqrt{2}}, \quad \lambda_4 = \sqrt{\frac{1}{2} - \lambda_3^2}.$$

Thus, only one variable, say λ_3, is needed to parametrize the lower boundary. The pairwise concurrences in such states are $C_{12} = \sqrt{2}\,\lambda_3$, $C_{13} = 0$, and $C_{23} = 0$. The states, using instead of λ_3, the entanglement C_{12}, are given by

$$|\psi_{\mathrm{M3TS}}\rangle = \frac{1}{\sqrt{2}}\left(|000\rangle + C_{12}|110\rangle + \sqrt{1 - C_{12}^2}|111\rangle\right). \quad (27)$$

These are explicit forms of maximally-3-tangled states. If $C_{12} = 0$, this results in the three-qubit GHZ states. For $C_{12} = 1$ it reduces to $(|00\rangle + |11\rangle)|0\rangle/\sqrt{2}$, wherein qubits 1 and 2 are maximally entangled and qubit 3 is not entangled to them.

The 3-tangle for $|\psi_{\mathrm{M3TS}}\rangle$ states are

$$\tau = 1 - C_{12}^2 = 1 - R_{12}^4. \quad (28)$$

In Fig. 2, the 3-tangle τ is plotted as a function of entanglement between qubits 1 and 2 (C_{12}) for a random sampling of three-qubit states. It is clear that the states in Eq. (27) give the maximum 3-tangle for the given value of C_{12}. Also, as a consequence of this maximization it is found that $C_{13} = C_{23} = 0$ for these states, which is a reflection of the monogamy of entanglement. When the entanglement between two qubits in a tripartite system is held fixed, maximizing the multipartite entanglement results in the other two pairs not being entangled.

For these states it also holds that $R_{23} = R_{13} = 0$. Indeed, the reduced density matrices are

$$\rho_{13} = \rho_{23} = \tfrac{1}{2}(|1\rangle\langle 1| \otimes |\alpha\rangle\langle\alpha| + |0\rangle\langle 0| \otimes |0\rangle\langle 0|), \quad (29)$$

where

$$|\alpha\rangle = C_{12}|0\rangle + \sqrt{1 - C_{12}^2}|1\rangle.$$

It is quite clear that these are classical-quantum correlated states as in Eq. (16) and it has been shown already in Sec. II that R_{13} and R_{23} indeed vanish for this class. On the other hand, the reduced density matrix of the first and the second qubits is a mixture of two Bell states

$$\rho_{12} = \left(\frac{1+C_{12}}{2}\right)|\phi^+\rangle\langle\phi^+| + \left(\frac{1-C_{12}}{2}\right)|\phi^-\rangle\langle\phi^-|, \quad (30)$$

therefore, a special case of Bell-diagonal states [12,33].

A natural generalization of $|\psi_{\mathrm{M3TS}}\rangle$ presents itself as states whose 3-tangle is maximized under constraints that two of the pair entanglements are fixed, say, C_{12} and C_{13}. Stationary points of the 3-tangle with these constraints lead to $(\lambda_0 = 1/\sqrt{2}, \lambda_1 = 0, \lambda_2 = C_{13}/\sqrt{2}, \lambda_3 = C_{12}/\sqrt{2})$ and can be shown to be a maxima. Thus, the states have two parameters and are given as follows:

$$|\psi\rangle = \frac{1}{\sqrt{2}}\big(|000\rangle + C_{13}|101\rangle + C_{12}|110\rangle + \sqrt{1-C_{12}^2-C_{13}^2}|111\rangle\big), \quad (31)$$

and the 3-tangle τ of these states is given as follows:

$$\tau = 1 - C_{12}^2 - C_{13}^2. \quad (32)$$

Thus, the coefficients C_{12} and C_{13} have to be chosen such that $0 \leqslant C_{12}^2 + C_{13}^2 \leqslant 1$. Here, $C_{12} = \sqrt{2}\lambda_3$, $C_{13} = \sqrt{2}\lambda_2$, and interestingly it is found that $C_{23} = C_{12}C_{13}$. The states in Eq. (31) are natural generalizations of the M3TS. Contrary to the M3TS case, if the entanglement (concurrences) between first and second qubits, and between first and third qubits, is kept fixed at some nonzero value, then the maximization of the 3-tangle does not lead to zero entanglement (concurrence) between the second and third qubits. For these states it can be seen that $R_{12} = \sqrt{C_{12}}(1-C_{13}^2)^{1/4}$, $R_{13} = \sqrt{C_{13}}(1-C_{12}^2)^{1/4}$, and $R_{23} = \sqrt{C_{12}C_{13}}(1-C_{12}^2)^{1/4}(1-C_{13}^2)^{1/4}$, so that $R_{23} = R_{12}R_{13}$ as well. These expressions reduce to those of M3TS for $C_{13} = 0$. For other interpretations and appearance of the M3TS, please see the last section.

IV. TWO-QUBIT STATES WITH RANK > 2

For rank-1 and -2 states, or pure two-qubit and pure three-qubit states, the connections between the measure R_{12} derived from the partial transpose followed by realignment and standard entanglement measures such a concurrence, and 3-tangle is striking and instructive. It also leads naturally to a segregation of the W states, as well as to a class of states that are in an essential sense maximally tangled, the M3TS states. When we step beyond to rank-3 and -4 states, the picture predictably gets murkier. The purifications are, for example, to systems of two-qubits and a qutrit for the rank-3 case. Equivalents of 3-tangles are to our knowledge not readily available. Yet, from lower-rank cases we can expect that the difference of some powers of R_{12} and C_{12} may reflect multiparty entanglement present in such purifications. This expectation is predicated on the inequality $R_{12} \geqslant C_{12}$ continuing to hold for rank-3 and -4 cases, which appears to be true.

This was checked numerically in two ways. One, by direct Haar sampling of pure states of two-qubits and one-qutrit (rank-3 case) or one-ququad (rank-4 case), and constructing

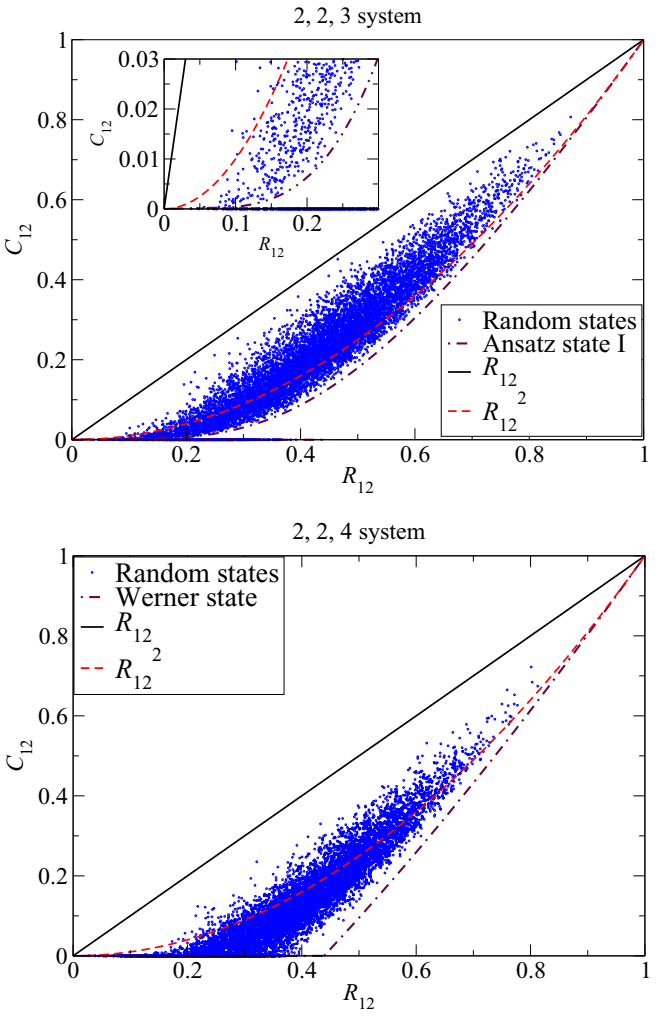

FIG. 3. The R_{12} and the entanglement between two qubits C_{12} having density matrix ρ_{12} of rank 3 and 4 at top and bottom, respectively. Also shown are the boundaries for rank-2 states for comparison. Ansatz-state-I curve in top figure corresponds to Eqs. (35) and (36). Werner state curve in the bottom figure corresponds to Eq. (39). Here, 10 000 random tripartite complex pure states with respective dimension of the third subsystem are used. The insets show an enlarged view of the region near the origin in the top figure.

R_{12} and C_{12}. The result is shown in Fig. 3 where only rank-3 and rank-4 cases are shown. It is clear that the straight line corresponding to $C_{12} = R_{12}$ is being typically avoided, and in fact R_{12} versus C_{12} is quite large. States close to the equality line are therefore all rank-1 and some rank-2 states. This is in accordance with the picture that emerged of the difference being a multiparty entanglement of the purification. We expect that there is more of such entanglement present in purifications of rank-3 or rank-4 states. Note that the latter can also be thought of reduced density matrices of four-qubit pure states.

The second method by which this was checked was by explicitly constructing the density matrix ρ_{12} (real case) in its spectrally decomposed form, where its four eigenvectors and eigenvalues are parametrized. Then, with these parametrized eigenvalues and eigenvectors, and using *Mathematica* 9, it is checked that the density matrix ρ_{12} satisfies $R_{12} \geqslant C_{12}$.

Thus, it is proved for real rank-4 two-qubit density matrices $R_{12} \geqslant C_{12}$ and it is most likely valid for complex states as well. Considering arbitrary rank-4 perturbations of pure states also validated this inequality. Further, in this regard see the comment at the end of the paper.

A. States in the lower boundary of the rank-3 case

States that give the lower boundaries in Fig. 3 for ranks 3 and 4 are now discussed. They are assumed to be mixtures of Bell states as was the lower boundary of the rank-2 case, namely, the reduced density matrix of M3TS states. Consider first the case of rank 3, for which an ansatz for the states in the lower boundary is

$$\rho_{12} = \frac{1-p}{2}\left(|\psi^+\rangle\langle\psi^+| + |\psi^-\rangle\langle\psi^-|\right) + p\,|\phi^+\rangle\langle\phi^+|. \quad (33)$$

This will be referred to as "ansatz state I" in the following. It is readily verified that

$$C_{12} = \max\{0, 2p-1\}, \quad R_{12} = \sqrt{p}\,|2p-1|^{1/4}. \quad (34)$$

For $0 \leqslant p \leqslant 1/2$, the concurrence is zero, however, R_{12} increases from 0 to a maximum value of $(1/3)^{3/4}$ when $p = 1/3$, and decreases again to zero at $p = 1/2$. Thus, there are two distinct segments in the R_{12} versus C_{12} graph for this state, one a horizontal segment

$$C_{12} = 0 \;\text{ for }\; 0 \leqslant R_{12} \leqslant (1/3)^{3/4}, \quad (35)$$

and the other the curve

$$R_{12} = C_{12}^{1/4}\sqrt{\frac{1+C_{12}}{2}}, \quad (36)$$

when $1/2 < p \leqslant 1$. Both these segments are shown in Fig. 3 where the regions

$$\begin{gathered} C_{12} < R_{12} \leqslant C_{12}^{1/4}\sqrt{\frac{1+C_{12}}{2}} \quad \text{for} \quad C_{12} > 0, \\ 0 \leqslant R_{12} \leqslant (1/3)^{3/4} \;\text{ for }\; C_{12} = 0 \end{gathered} \quad (37)$$

are populated.

Apart from this figure, strong evidence that the lower boundary is indeed given by states in Eq. (33) is checked numerically by adding a random density matrix ρ_R to this ansatz such that the resultant state is still of rank 3. This random density matrix is such that its eigenvalues are chosen randomly with eigenvectors as $|\psi^\pm\rangle$ and $|\phi^+\rangle$ such that the final density matrix is of rank 3 with unaltered eigenvectors. The eigenvalues are selected as $\cos^2(\theta)$, $\sin^2(\theta)\cos^2(\phi)$, and $\sin^2(\theta)\sin^2(\phi)$ where θ and ϕ are independent random variables chosen uniformly from $[0,\pi]$ and $[0,2\pi]$, respectively. The final density matrix ρ'_{12} is given as follows:

$$\rho'_{12} = \frac{\rho_{12} + \varepsilon\rho_R}{1+\varepsilon}, \quad (38)$$

where ρ_{12} is the ansatz state and ε is the perturbation parameter which controls the amount of randomness added to the ansatz state ρ_{12}. In Fig. 4, results are shown for states generated as per Eq. (38) for various values of ε. It can be seen from the figure (and was also checked numerically) that there is no violation of Eqs. (37). A more general rank-3 state which lies close to the subspace spanned by $\{|\psi^\pm\rangle, |\phi^+\rangle\}$ may be constructed by Gram-Schmidt orthonormalization. Results not presented here reconfirm that the boundary is populated with states as in Eq. (33).

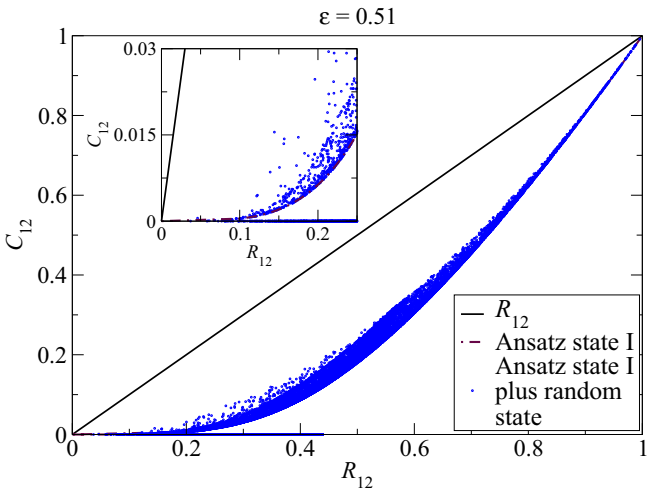

FIG. 4. The R_{12} and the entanglement between two-qubits C_{12} having density matrix ρ'_{12} of rank 3 given in Eq. (38) for $\varepsilon = 0.51$. Here, 20 000 such states are sampled randomly in each case. Also shown are the bounds from Eqs. (37). The insets show an enlarged view of the region near the origin.

B. Werner states form the lower boundary in the rank-4 case

Evidence is now presented that Werner states form the lower boundary of rank-4 density matrices, and hence the whole $C_{12} - R_{12}$ diagram. Just as in rank-2 and rank-3 cases, these border states are also Bell diagonal. Consider the Werner state $\rho_W = (1-p)I/4 + p\,|\psi^-\rangle\langle\psi^-|$ [35] $(0 \leqslant p \leqslant 1)$, which is entangled iff $1/3 < p \leqslant 1$ and in that case the entanglement, as measured by the concurrence, is $C_{12} = (3p-1)/2$. As mentioned in the Introduction, $R_{12} = p^{3/4}$ for these states. Substituting p in terms of R_{12} in the expression for concurrence one obtains the following:

$$C_{12} = \max\left\{0, \frac{3R_{12}^{4/3} - 1}{2}\right\}. \quad (39)$$

Thus, $C_{12} = 0$ for $0 \leqslant R_{12} \leqslant (1/3)^{3/4}$ which is also the case for the ansatz given for rank-3 border states [refer Eq. (37)]. It is greater than zero for $(1/3)^{3/4} < R_{12} \leqslant 1$, in which case $R_{12} = [(2C_{12}+1)/3]^{3/4}$. This curve is plotted in that part of Fig. 3 that corresponds to rank-4 states.

To check that Eq. (39) indeed forms the lower boundary for the rank-4 cases, again random perturbations are added to the border (Werner) states. First a random tripartite pure is selected consisting of two-qubits and a ququad. The reduced density matrix of the two-qubits ρ_R is then added to the Werner state:

$$\rho_{12} = (\rho_W + \varepsilon\rho_R)/(1+\varepsilon). \quad (40)$$

It can be seen from Fig. 5 (and also verified numerically) that there are no states that violate the inequality in Eq. (39). Thus, for the rank-4 case (and hence for generic two-qubit states) it

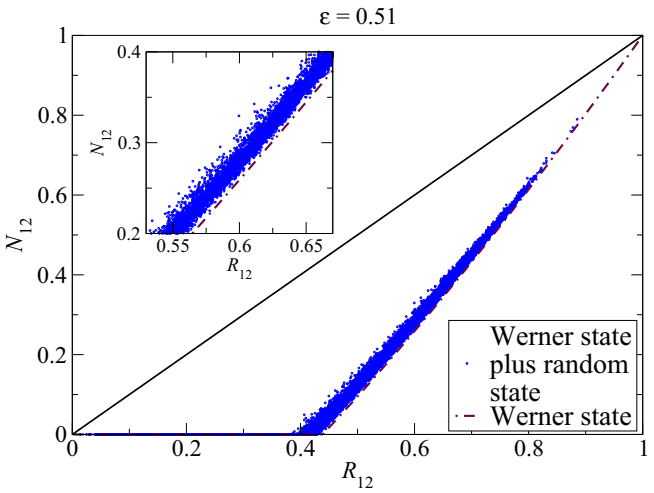

FIG. 5. The R_{12} and the entanglement between two-qubits C_{12} having density matrix ρ'_{12} of rank 4 given in Eq. (40) for values of $\varepsilon = 0.51$. Here, 20 000 such states are sampled randomly in each case. Werner state curve corresponds to Eq. (39). Also shown are the bounds from Eq. (39). The insets show an enlarged view of the region around $R_{12} = 0.6$ and $N_{12} = 0.3$.

follows that

$$C_{12} \leqslant R_{12} \leqslant \left(\frac{2C_{12}+1}{3}\right)^{3/4} \quad \text{for} \quad C_{12} \geqslant 0. \tag{41}$$

In Fig. 6, the various boundaries of the $C_{12} - R_{12}$ diagram are shown for arbitrary two-qubit states. It includes the parabola from Proposition 2, and curves from Eqs. (37) and (41). The curve corresponding to rank 1 is the common upper boundary for all the ranks, and is simply the line $C_{12} = R_{12}$. It can be seen that as the rank increases, the corresponding lower boundary gets shifted in the downward direction, but always remains a Bell-diagonal state.

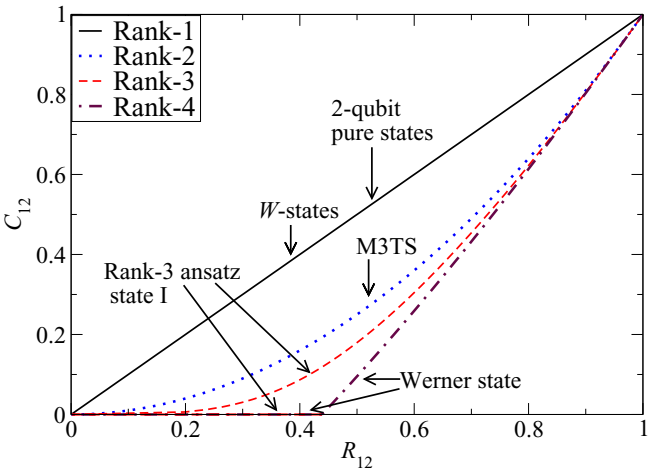

FIG. 6. Boundary curves for R_{12} and the entanglement between two-qubits C_{12} having density matrix ρ_{12} of all the ranks as per given in Proposition 2 [Eqs. (37) and (41)]. Also shown are various classes of states lying on the respective boundaries.

C. Concurrence and R_{12} in X states

An important subset of two-qubit states are the so-called X states [58–61] which appear in many physical contexts from quantum optics to condensed matter [61–63]. They have been intensively investigated, and there are analytical formulas for the quantum discord of the X states [60,61], which were later shown to have very small worst-case error by giving explicit counterexamples [64]. It is therefore of interest to investigate them in the context of this paper, especially as they are in general of full rank. The states are given by the following form that makes the sobriquet "X states" evident:

$$\rho_X = \begin{pmatrix} a & 0 & 0 & w \\ 0 & b & z & 0 \\ 0 & z^* & c & 0 \\ w^* & 0 & 0 & d \end{pmatrix}. \tag{42}$$

This describes a quantum state provided the unit trace and positivity conditions $a + b + c + d = 1$, $\sqrt{bc} \geqslant |z|$, $\sqrt{ad} \geqslant |w|$ are satisfied. X states are entangled if and only if either $\sqrt{bc} \leqslant |w|$ or $\sqrt{ad} \leqslant |z|$, and both conditions cannot hold simultaneously [65]. Concurrence is $C_{12} = 2\max\{0, |z| - \sqrt{ad}, |w| - \sqrt{bc}\}$. For X states, it is readily seen that

$$R_{12} = 2|ad - bc|^{1/4}||z|^2 - |w|^2|^{1/4}, \tag{43}$$

which has an interesting structure, involving the product of the determinants of the reshaped diagonal and antidiagonal.

Proposition 3. For X states, $R_{12} \geqslant C_{12}$.

Proof. That

$$|ad - bc|^{1/4} \geqslant ||w|^2 - bc|^{1/4},$$
$$||w|^2 - |z|^2|^{1/4} \geqslant ||w|^2 - bc|^{1/4},$$

follow from the conditions that $\sqrt{ad} \geqslant |w|$ and $|z| \leqslant \sqrt{bc}$, respectively. It follows then that

$$R_{12} \geqslant 2\,||w|^2 - bc|^{1/2}, \quad R_{12} \geqslant 2\,||z|^2 - ad|^{1/2},$$

the latter being derived similarly. However, it also follows easily that $||w|^2 - bc|^{1/2} \geqslant |w| - \sqrt{bc}$ provided $|w| \geqslant \sqrt{bc}$ and similarly $||z|^2 - ad|^{1/2} \geqslant |z| - \sqrt{ad}$ when $|z| \geqslant \sqrt{ad}$. Thus, whenever the concurrence is nonzero, it is necessarily smaller than or equal to R_{12}. ■

As a simple corollary, whenever $R_{12} = 0$, then $C_{12} = 0$. For X states, it is clear that $R_{12} = 0$ whenever $ad = bc$ or $|w| = |z|$. It is not evident from the concurrence expressions that it is zero in these cases, but it is so.

V. NEGATIVITY AND R_{12}

While the R_{12}-concurrence pair has been exhaustively studied in the case of two-qubit states, it is interesting to compare R_{12} with other measures of entanglement. In particular, as R_{12} is crucially dependent on the partial transpose operation, it is of interest to compare it with "negativity" [66–68] which is exclusively based on the partial transpose operation.

For a two-qubit state ρ_{12}, after partial transpose, at most only one eigenvalue can be negative. The negativity is then defined as

$$N(\rho_{12}) = \max\{0, -2\mu_{\min}\}, \tag{44}$$

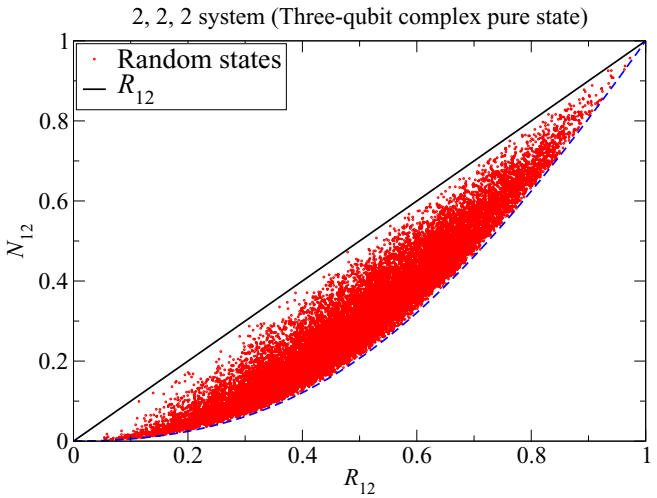

FIG. 7. The R_{12} and the negativity between two-qubits N_{12} having density matrix ρ_{12} of rank 2. Also shown are various analytical curves. The lower curve corresponds to the lower boundary in Eq. (46). Here, 20 000 random tripartite complex three-qubit pure states are used.

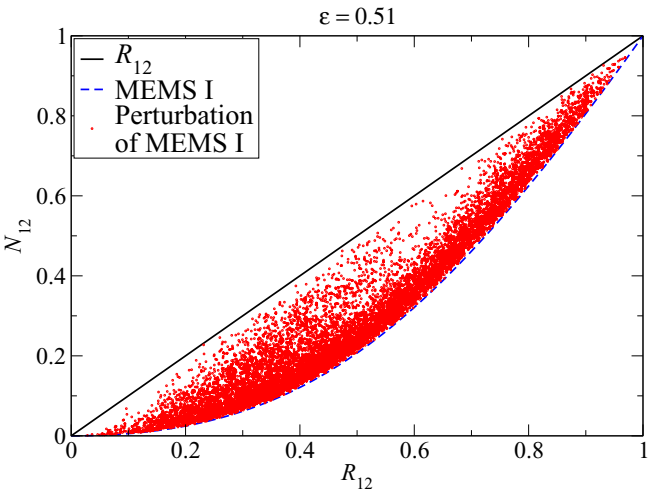

FIG. 8. The R_{12} and the negativity between two-qubits N_{12} having density matrix ρ_{12} obtained using Eq. (48). Parameter used is $\varepsilon = 0.51$. Here, 10 000 such states are selected.

where $\mu_{\min}$ is the minimum eigenvalue of the partial transpose of ρ_{12}. Unlike concurrence, negativity can be calculated for bipartite systems of any dimensionality. If the negativity is nonzero, then the state is entangled. In that case ρ_{12} is said to be a NPT (negative partial transpose) state, otherwise it is a PPT (positive partial transpose) state and is guaranteed to be separable only for 2×2 and 2×3 systems [69]. Concurrence and negativity for two-qubit states have been previously compared [33,67,70] and it was shown that the following holds:

$$\sqrt{(1 - C_{12})^2 + C_{12}^2} - (1 - C_{12}) \leqslant N_{12} \leqslant C_{12}. \qquad (45)$$

It was also shown that the class of states which satisfies the bound $N_{12} = C_{12}$ includes two-qubit pure states, and Bell-diagonal states [12,33] (which include Werner states) while the class of states which satisfy the lower bound are rank-2 maximally entangled mixed states of rank, i.e., MEMS I [33,36–39].

A. Rank-1 and -2 states

It should be noted that the inequality in Eq. (45) holds true for two-qubit density matrices of all ranks. However, as shown below, the same inequality, with R_{12} simply replacing C_{12}, holds true for the restricted class of two-qubit rank-1 or rank-2 states. That is, for these states

$$\sqrt{(1 - R_{12})^2 + R_{12}^2} - (1 - R_{12}) \leqslant N_{12} \leqslant R_{12}. \qquad (46)$$

To begin with, the inequality in Eq. (46) is checked for 100 000 random states ρ_{12} which are reduced density matrices of pure states of three-qubits that are drawn from the Haar measure. The bounds are found to hold true in every case, including in a subset which is shown in Fig. 7. The boundary states are now presented and verified to be boundaries by using perturbations as in the cases above.

1. *Pure states have $N_{12} = R_{12}$*

It can be seen easily that for any arbitrary two-qubit pure state $|\psi\rangle = a|00\rangle + b|01\rangle + c|10\rangle + d|11\rangle$, N_{12} and R_{12} are the same and given by $N_{12} = R_{12} = 2|ad - bc|$. Thus, all two-qubit pure states correspond to the upper boundary of Fig. 7. It is interesting that while apart from pure states, $C_{12} = R_{12}$ also for all (rank-2) reduced density matrices from the W class of three-qubit states, this is no longer the case when negativity is compared with R_{12}. Such states are found not to be special and fill the interior of the region in Fig. 7 rather uniformly.

2. *The lower boundary are MEMS I*

The R_{12}-concurrence lower boundary consisted of M3TS states. These do not form the border when negativity replaces the concurrence. It is easy to see that for M3TS states $N_{12} = R_{12}^2$. MEMS I [33,36–39] were special in the R_{12}-concurrence case and were the upper boundary as $C_{12} = R_{12}$. The spectral decomposition of MEMS I is

$$\rho_{\text{MEMS I}} = (1 - C_{12})|01\rangle\langle 01| + C_{12}|\phi^+\rangle\langle\phi^+|, \qquad (47)$$

where R_{12} can also be used in place of C_{12} owing to their equality for such states. Again, simple explicit calculations yield in this case that $N_{12} = \sqrt{(1 - R_{12})^2 + R_{12}^2} - (1 - R_{12})$, the lower bound in Eq. (46).

That these states turn out to form the lower boundary in the R_{12}-negativity case (restricted to rank-2 states) is established by using random rank-2 perturbations and the result is displayed in Fig. 8. The procedure of perturbation is now given. As proved in Sec. III B 1, MEMS I is the reduced density matrix of a subset of W class of states as given in Eq. (25). Using these three-qubit purifications of perturbations of MEMS I can be constructed as

$$|\phi\rangle = \frac{|\psi\rangle + \varepsilon|\psi_R\rangle}{\sqrt{1 + \varepsilon^2 + \varepsilon(\langle\psi|\psi_R\rangle + \langle\psi_R|\psi\rangle)}}. \qquad (48)$$

Here, $|\psi\rangle$ is a state in the W class restricted to the form in Eq. (25) (C_{12} uniformly random in [0,1]), and $|\psi_R\rangle$ is a three-qubit random pure state selected according to the Haar

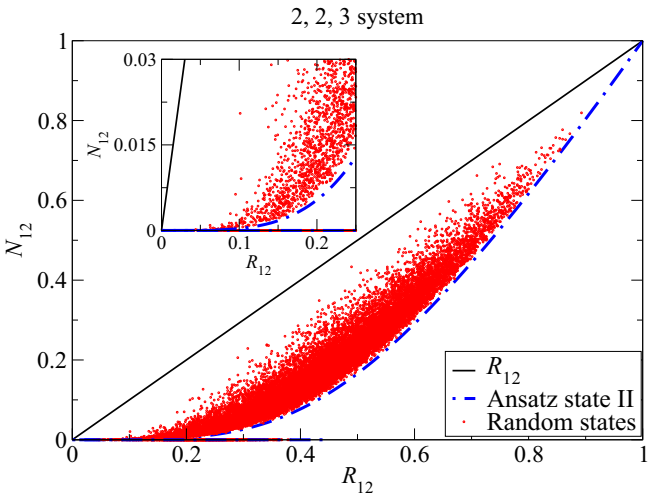

FIG. 9. The R_{12} and the negativity between two-qubits N_{12} having density matrix ρ_{12} of rank 3. Also shown are various analytical curves. Ansatz state II in the figure corresponds to Eq. (53). Here, 20 000 random tripartite complex pure states with respective dimension of the third subsystem are used. The insets show an enlarged view of the region near the origin.

measure and ε is the perturbation parameter. Results in Fig. 8 are presented for $\varepsilon = 0.51$. It can be seen that the inequality in Eq. (46) is strictly respected. A rather large value of the "perturbation" is used to clearly show the strict spread of the values to the left of the boundary curve.

B. Two-qubit states with rank > 2

For rank-3 and -4 states it is found from extensive numerical sampling that the lower bound in Eq. (46) is violated while the upper bound is still valid (refer Fig. 9). In other words, for rank 3 and rank 4, the inequality $N_{12} \leqslant R_{12}$ holds. Here too it can be seen that there is a lower bound on the spread of the states, i.e., for given value of N_{12} there seems to be a maximum value taken by R_{12} or for given value of R_{12} there is the minimum value taken by N_{12}.

1. States in the lower boundary of the rank-3 case

For the case of rank-3 states it is found that neither the ansatz state I given in Eq. (33) (which gave the lower boundary for the concurrence versus R_{12}) nor the MEMS II define the lower boundary of negativity versus R_{12}. Based on the fact that the spectral decomposition of MEMS I states which form the lower boundary of rank-2 states are mixtures of a pure separable state and an orthogonal maximally entangled state [Eq. (47)], the following generalization ("anstaz state II") is examined:

$$\rho_{12} = \alpha|01\rangle\langle 01| + \beta|\phi^+\rangle\langle\phi^+| + \gamma|\phi^-\rangle\langle\phi^-|, \tag{49}$$

where $0 \leqslant \alpha,\beta,\gamma \leqslant 1$ and $\alpha + \beta + \gamma = 1$. It is readily verified that for these states

$$R_{12} = \sqrt{|\beta^2 - \gamma^2|}, \quad N_{12} = \sqrt{\alpha^2 + (\beta - \gamma)^2} - \alpha. \tag{50}$$

The coefficients α,β and $\gamma = 1 - \alpha - \beta$ are now fixed such that for a given value of R_{12} the minimum value of negativity is obtained. Using the method of Lagrange multipliers with α as an independent parameter, this minimization fixes the other coefficients as

$$\begin{aligned} \beta &= \tfrac{1}{2}[1 - \alpha + \sqrt{(1-\alpha)(1-3\alpha)}], \\ \gamma &= \tfrac{1}{2}[1 - \alpha - \sqrt{(1-\alpha)(1-3\alpha)}]. \end{aligned} \tag{51}$$

It should be noted that $0 \leqslant \alpha \leqslant 1/3$ to have valid values of β and γ. With these values of the coefficients, the state in Eq. (49) is the ansatz state II for which using Eq. (50) one gets

$$R_{12} = (1-\alpha)^{3/4}(1-3\alpha)^{1/4}, \quad N_{12} = 1 - 3\alpha. \tag{52}$$

Hence, the corresponding negativity versus R_{12} curve is

$$R_{12} = N_{12}^{1/4}\left(\frac{2 + N_{12}}{3}\right)^{3/4}, \tag{53}$$

which is indeed found to be the lower boundary in Fig. 9.

As for any two-qubit state $N_{12} = 0$ if and only if $C_{12} = 0$ it follows that the ansatz state I given in Eq. (33), with $0 \leqslant p \leqslant 1/2$, belongs to the horizontal segment with $N_{12} = 0$ in Fig. 9. As in that case, the maximum value of R_{12} for rank-3 states with $N_{12} = 0$ is $(1/3)^{3/4}$. To summarize, the regions

$$\begin{aligned} &N_{12} < R_{12} \leqslant N_{12}^{1/4}\left(\frac{2 + N_{12}}{3}\right)^{3/4} \quad \text{for} \quad N_{12} > 0, \\ &\text{and} \quad 0 \leqslant R_{12} \leqslant (1/3)^{3/4} \quad \text{for} \quad N_{12} = 0 \end{aligned} \tag{54}$$

are populated for rank-3 states. It is checked numerically (results not presented) that perturbing the boundary states always results in values of negativity and R_{12} that lie in the interior of this region. Thus, although the properties of MEMS I motivated the form of the ansatz state II for nonzero negativity in the rank-3 case, it should be noted that this is different from the rank-3 MEMS II [33,36–39].

2. Werner states are in the lower boundary of rank-4 cases

Evidence is now presented that Werner states form the lower boundary of full-rank states. As the Werner state is a Bell-diagonal state, $C_{12} = N_{12}$ [12,33], and it follows on using Eq. (39) that

$$N_{12} = \max\left\{0, \frac{3R_{12}^{4/3} - 1}{2}\right\}. \tag{55}$$

It can be seen that N_{12} is zero for $0 \leqslant R_{12} \leqslant (1/3)^{3/4}$ which is also the case of rank-3 border states [refer Eq. (54)]. It is greater than zero for $(1/3)^{3/4} < R_{12} \leqslant 1$, in which case $N_{12} = (3R_{12}^{4/3} - 1)/2$ or equivalently $R_{12} = [(2N_{12} + 1)/3]^{3/4}$. This curve is shown in Fig. 10 along with results from rank-4 matrices derived from a Haar sampling of pure states in (2,2,4) dimensions.

To check that Eq. (55) indeed forms the lower boundary for rank-4 case in Fig. 10, the same method from Sec. IV B is employed. Results not presented here then confirm that the Werner states lie on the boundary of the R_{12} versus negativity region and define the extreme curve within which all states lie. To summarize, for all two-qubit states, including the

rank-4 case,

$$N_{12} \leqslant R_{12} \leqslant \left(\frac{2N_{12}+1}{3}\right)^{3/4} \quad \text{for} \quad N_{12} \geqslant 0. \tag{56}$$

In Fig. 11, the boundary curves corresponding to all the ranks of two-qubit density matrices are shown. It includes various analytical curves from Eqs. (46), (53), and (55). The curve corresponding to rank 1 is common to all the ranks. It can be seen that as the rank increases, the corresponding lower boundaries get lower. If a two-qubit state is separable, then $N_{12} = C_{12} = 0$, and in this case the maximum value of R_{12} is $(1/3)^{3/4} \approx 0.4387$. In other words, if for a two-qubit state $R_{12} > (1/3)^{3/4}$, it is necessarily entangled. If this criterion is applied to, for example, Werner state it gives clear separable-entangled regions.

It should be noted that throughout this work, possible classes of states with respective boundaries are given and verified with various numerical and analytical methods, but apart from these there could be other classes of states on the boundaries.

VI. SUMMARY AND DISCUSSIONS

In this paper, correlations in bipartite density matrices on $\mathcal{H}^d \otimes \mathcal{H}^d$ were studied using the quantity $R_{12} = d|\det[\mathcal{R}(\rho_{12}^{T_2})]|^{1/d^2}$, where $\mathcal{R}(\rho_{12}^{T_2})$ is formed by the combined operations of partial transpose and realignment on the density matrix. It is based on a simple permutation of the density matrix and involves no extremization, or even diagonalization. It is proved that $0 \leqslant R_{12} \leqslant 1$. Several examples show how they vanish on large classes of separable states including classical-quantum correlated states, while being maximum

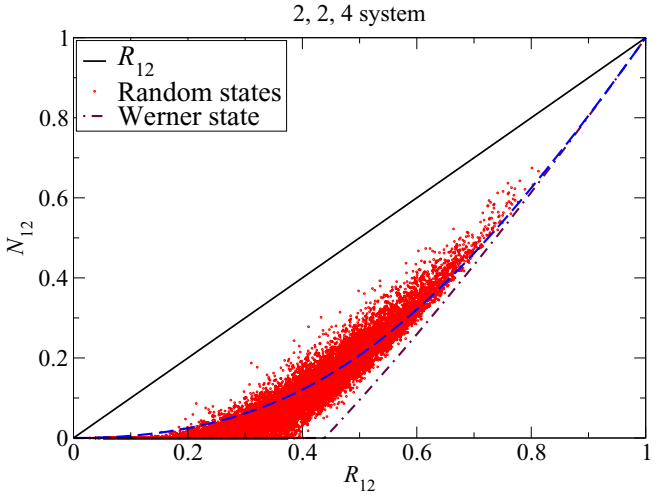

FIG. 10. The R_{12} and the negativity between two-qubits N_{12} having density matrix ρ_{12} of rank 4. Also shown are various analytical curves. The dashed curve in the figure corresponds to the lower boundary in Eq. (46). The Werner state curve in the bottom figure corresponds to Eq. (55). Here, 20 000 random tripartite complex pure states with respective dimension of the third subsystem are used.

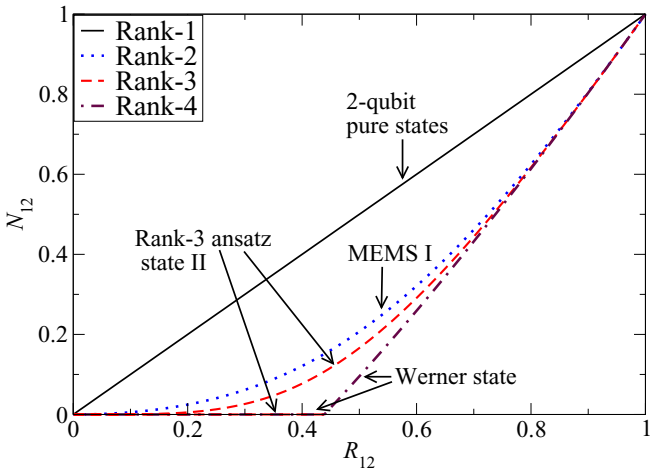

FIG. 11. Boundary curves for R_{12} and the entanglement between two-qubits N_{12} having density matrix ρ_{12} of all the ranks as per given in Eqs. (46), (54), and (56). Also shown are various classes of states lying on the respective boundaries.

(= 1) on maximally entangled states. It is also shown that R_{12} is an entanglement monotone only on two-qubit pure states since in this case it equals concurrence as well as negativity. These properties are reminiscent of quantum discord. Two-qubit density matrices were studied in detail to motivate that this measure captures entanglement in the bipartite state along with other multiparty entanglement that may be present in the purification of such states.

In the case of density matrices of rank 2, their purification in terms of three-qubit states is possible. Extensive use of the canonical form of three-qubit pure state is made to make simple connections between R_{12}, the concurrence, and the tripartite measure of the 3-tangle. When the density matrix is of rank 2, analytical results on the lower and upper bounds of the concurrence in terms of R_{12} are obtained. States satisfying the bounds are found to be special, one being the well-known W states, and the other (see comments below) referred to here as maximally-3-tangled states (M3TS) as they have the property of maximizing the tripartite entanglement for a given entanglement (concurrence) between two-qubits. It is found that this maximization leads to zero entanglement in the other two pairs, reflecting the monogamy of entanglement.

Interestingly, if the entanglement between two pairs of qubits in a tripartite pure state are kept fixed, then the maximization of the 3-tangle does not lead to zero entanglement between the second and the third qubits and leads to a generalization of the M3TS. In the case of two-qubit density matrices of ranks 3 and 4, strong evidence is provided that $R_{12} \geqslant C_{12}$. The physically important subset of X states, which are of rank 4 in general, is considered where this is explicitly proved. Upper bounds on R_{12} and the class of states satisfying these bounds are given for all higher ranks as well. As in the case of rank 2, the boundary states are Bell diagonal (whose purification is the M3TS) in the case of rank 3 also it is a Bell-diagonal state, which has been identified and verified numerically. For the rank-4 states, the border states are Werner states, which are also special cases of Bell-diagonal

states. Thus, the R_{12} versus concurrence "phase diagram" is an interesting one which has many special states at the boundaries separating states by rank.

Apart from concurrence, another important measure, namely the negativity, has been compared with R_{12} for two-qubit density matrices. Motivations are that negativity, unlike concurrence, can be defined in arbitrary dimensional systems, and it is also derived from the operation of partial transpose. Upper and lower bounds on R_{12} in terms of negativity and the class of states satisfying these bounds are given for all the ranks. In the case of rank 2, the state is given by MEMS I, for rank 3 the state is a mixture of two Bell states and a separable pure state orthogonal to both of them. While in the case of rank 4, the ansatz state is again the Werner state. Strong evidences are provided in support of these boundaries and the ansatz states satisfying them.

Recently, we have come to know of various related aspects of the central quantity R_{12} and the states M3TS. In the two-qubit case, the inequality $R_{12} \geqslant C_{12}$ is established analytically [31,32]. The M3TS states have been studied as "maximal slice" [44] states and have been shown to violate maximally, for a given tangle, a tripartite nonlocality inequality, namely, the Svetlichny inequality [50,71]. However, the rather simple and natural way in which it appears on maximizing the 3-tangle for a given concurrence (or R_{12}) is interesting.

Thus, there is a significance associated with most of the boundary states and hence makes R_{12} an interesting quantity for more detailed investigation. In particular, every two-qubit pure state violates Bell's inequality [72], the M3TS violates the Svetlichny inequality, W class of states have zero 3-tangle [51], Werner states have maximum negativity for given linear entropy, while MEMS I have maximum concurrence for given linear entropy [33,36–39]. It will be interesting to investigate the significance of the ansatz states I and II. Considering other spectral quantities than the determinant of $\mathcal{P}(12)$ is possible. More detailed studies and interpretation of such quantities is of interest, and it is hoped that this work provides sufficient reasons and motivations.

ACKNOWLEDGMENTS

We are very grateful to Antony Milne for bringing our attention to the relationship of R_{12} to "obesity", and to Shohini Ghose for pointing out that the M3TS states have previously been studied as the maximal slice states. We are also grateful to Karol Życzkowski for comments about higher-rank boundary states, and thank an anonymous referee for suggesting the comparison of negativity and R_{12}. U.T.B. is happy to acknowledge many discussions with M. S. Santhanam and T. S. Mahesh. He would like to acknowledge the funding received from Department of Science and Technology, India under the scheme Science and Engineering Research Board (SERB) National Post Doctoral Fellowship (NPDF) file Number PDF/2015/00050.

[1] R. Horodecki, P. Horodecki, M. Horodecki, and K. Horodecki, Rev. Mod. Phys. **81**, 865 (2009).
[2] C. H. Bennett, G. Brassard, C. Crépeau, R. Jozsa, A. Peres, and W. K. Wootters, Phys. Rev. Lett. **70**, 1895 (1993).
[3] C. H. Bennett and G. Brassard, in *Proceedings of IEEE International Conference on Computers, Systems, and Signal Processing, Bangalore, India* (IEEE, New York, 1984), pp. 175–179.
[4] M. Żukowski, A. Zeilinger, M. A. Horne, and A. K. Ekert, Phys. Rev. Lett. **71**, 4287 (1993).
[5] S. Bose, V. Vedral, and P. L. Knight, Phys. Rev. A **57**, 822 (1998).
[6] C. H. Bennett, D. P. DiVincenzo, P. W. Shor, J. A. Smolin, B. M. Terhal, and W. K. Wootters, Phys. Rev. Lett. **87**, 077902 (2001).
[7] C. H. Bennett and S. J. Wiesner, Phys. Rev. Lett. **69**, 2881 (1992).
[8] M. Piani and J. Watrous, Phys. Rev. Lett. **102**, 250501 (2009).
[9] W. Dür, H.-J. Briegel, J. I. Cirac, and P. Zoller, Phys. Rev. A **59**, 169 (1999).
[10] C. H. Bennett, H. J. Bernstein, S. Popescu, and B. Schumacher, Phys. Rev. A **53**, 2046 (1996).
[11] W. K. Wootters, Quantum Inf. Comput. **1**, 27 (2001).
[12] W. K. Wootters, Phys. Rev. Lett. **80**, 2245 (1998).
[13] S. Hill and W. K. Wootters, Phys. Rev. Lett. **78**, 5022 (1997).
[14] A. Peres, Phys. Rev. Lett. **77**, 1413 (1996).
[15] M. Horodecki, P. Horodecki, and R. Horodecki, Phys. Rev. Lett. **80**, 5239 (1998).
[16] M. B. Plenio, Phys. Rev. Lett. **95**, 090503 (2005).
[17] H. Ollivier and W. H. Zurek, Phys. Rev. Lett. **88**, 017901 (2001).
[18] W. H. Zurek, Ann. Phys. (Berlin) **9**, 855 (2000).
[19] M. B. Plenio and S. Virmani, Quantum Inf. Comput. **7**, 1 (2007).
[20] A. Sawicki, M. Oszmaniec, and M. Kuś, Phys. Rev. A **86**, 040304 (2012).
[21] M. Walter, B. Doran, D. Gross, and M. Christandl, Science **340**, 1205 (2013).
[22] A. Sawicki, M. Oszmaniec, and M. Kuś, Rev. Math. Phys. **26**, 1450004 (2014).
[23] F. Verstraete, J. Dehaene, B. De Moor, and H. Verschelde, Phys. Rev. A **65**, 052112 (2002).
[24] K. Chen and L.-A. Wu, Quantum Inf. Comput. **3**, 193 (2003).
[25] O. Rudolph, Lett. Math. Phys. **70**, 57 (2004).
[26] O. Rudolph, Phys. Rev. A **67**, 032312 (2003).
[27] U. T. Bhosale, K. V. Shuddhodan, and A. Lakshminarayan, Phys. Rev. A **87**, 052311 (2013).
[28] M. S. Williamson, M. Ericsson, M. Johansson, E. Sjöqvist, A. Sudbery, V. Vedral, and W. K. Wootters, Phys. Rev. A **83**, 062308 (2011).
[29] V. Coffman, J. Kundu, and W. K. Wootters, Phys. Rev. A **61**, 052306 (2000).
[30] S. Jevtic, M. Pusey, D. Jennings, and T. Rudolph, Phys. Rev. Lett. **113**, 020402 (2014).
[31] A. Milne, D. Jennings, S. Jevtic, and T. Rudolph, Phys. Rev. A **90**, 024302 (2014).
[32] A. Milne, S. Jevtic, D. Jennings, H. Wiseman, and T. Rudolph, New J. Phys. **16**, 083017 (2014).
[33] F. Verstraete, K. Audenaert, and B. De Moor, Phys. Rev. A **64**, 012316 (2001).

[34] R. Horodecki and M. Horodecki, Phys. Rev. A **54**, 1838 (1996).
[35] R. F. Werner, Phys. Rev. A **40**, 4277 (1989).
[36] S. Ishizaka and T. Hiroshima, Phys. Rev. A **62**, 022310 (2000).
[37] W. J. Munro, D. F. V. James, A. G. White, and P. G. Kwiat, Phys. Rev. A **64**, 030302 (2001).
[38] T.-C. Wei, K. Nemoto, P. M. Goldbart, P. G. Kwiat, W. J. Munro, and F. Verstraete, Phys. Rev. A **67**, 022110 (2003).
[39] N. A. Peters, J. B. Altepeter, D. A. Branning, E. R. Jeffrey, T.-C. Wei, and P. G. Kwiat, Phys. Rev. Lett. **92**, 133601 (2004).
[40] M. Piani, V. Narasimhachar, and J. Calsamiglia, New J. Phys. **16**, 113001 (2014).
[41] S. Luo, Phys. Rev. A **77**, 042303 (2008).
[42] K. Modi, Open Syst. Inf. Dyn. **21**, 1440006 (2014).
[43] K. Modi, A. Brodutch, H. Cable, T. Paterek, and V. Vedral, Rev. Mod. Phys. **84**, 1655 (2012).
[44] H. A. Carteret and A. Sudbery, J. Phys. A: Math. Gen. **33**, 4981 (2000).
[45] A. Acín, A. Andrianov, L. Costa, E. Jané, J. I. Latorre, and R. Tarrach, Phys. Rev. Lett. **85**, 1560 (2000).
[46] A. Sudbery, J. Phys. A: Math. Gen. **34**, 643 (2001).
[47] A. Acín, A. Andrianov, E. Jané, and R. Tarrach, J. Phys. A: Math. Gen. **34**, 6725 (2001).
[48] R. Lohmayer, A. Osterloh, J. Siewert, and A. Uhlmann, Phys. Rev. Lett. **97**, 260502 (2006).
[49] C. Eltschka, A. Osterloh, J. Siewert, and A. Uhlmann, New J. Phys. **10**, 043014 (2008).
[50] S. Ghose, N. Sinclair, S. Debnath, P. Rungta, and R. Stock, Phys. Rev. Lett. **102**, 250404 (2009).
[51] W. Dür, G. Vidal, and J. I. Cirac, Phys. Rev. A **62**, 062314 (2000).
[52] C. Eltschka and J. Siewert, Phys. Rev. Lett. **108**, 020502 (2012).
[53] J. Siewert and C. Eltschka, Phys. Rev. Lett. **108**, 230502 (2012).
[54] S. Lee, J. Joo, and J. Kim, Phys. Rev. A **72**, 024302 (2005).
[55] S. Tamaryan, T.-C. Wei, and D. Park, Phys. Rev. A **80**, 052315 (2009).
[56] A. Ajoy and P. Rungta, Phys. Rev. A **81**, 052334 (2010).
[57] D. M. Greenberger, M. Horne, and A. Zeilinger, in *Bell's Theorem, Quantum Theory, and Conceptions of the Universe*, edited by M. Kafatos (Kluwer, Dordrecht, 1989), p. 69.
[58] T. Yu and J. H. Eberly, Quantum Inf. Comput. **7**, 459 (2007).
[59] A. R. P. Rau, J. Phys. A: Math. Theor. **42**, 412002 (2009).
[60] M. Ali, A. R. P. Rau, and G. Alber, Phys. Rev. A **81**, 042105 (2010).
[61] F. F. Fanchini, T. Werlang, C. A. Brasil, L. G. E. Arruda, and A. O. Caldeira, Phys. Rev. A **81**, 052107 (2010).
[62] T. Werlang, C. Trippe, G. A. P. Ribeiro, and G. Rigolin, Phys. Rev. Lett. **105**, 095702 (2010).
[63] M. S. Sarandy, Phys. Rev. A **80**, 022108 (2009).
[64] Y. Huang, Phys. Rev. A **88**, 014302 (2013).
[65] A. Sanpera, R. Tarrach, and G. Vidal, Phys. Rev. A **58**, 826 (1998).
[66] K. Życzkowski, P. Horodecki, A. Sanpera, and M. Lewenstein, Phys. Rev. A **58**, 883 (1998).
[67] J. Eisert and M. B. Plenio, J. Mod. Opt. **46**, 145 (1999).
[68] G. Vidal and R. F. Werner, Phys. Rev. A **65**, 032314 (2002).
[69] M. Horodecki, P. Horodecki, and R. Horodecki, Phys. Lett. A **223**, 1 (1996).
[70] A. Miranowicz and A. Grudka, Phys. Rev. A **70**, 032326 (2004).
[71] G. Svetlichny, Phys. Rev. D **35**, 3066 (1987).
[72] J. Bell, Physics **1**, 195 (1964).